Electronic Supplementary Information

Two-in-one: construction of hydroxyl and imidazolium-bifunctionalized ionic networks in one-pot toward synergistic catalytic CO_2 fixation

Yadong Zhang,[a] Guojian Chen,*[a,b] Lei Wu,[a] Ke Liu,[a] Hu Zhong,[a] Zhouyang Long,[a] Minman Tong,[a] Zhenzhen Yang[b,c] and Sheng Dai*[bc]

[a] School of Chemistry and Materials Science, Jiangsu Key Laboratory of Green Synthetic Chemistry for Functional Materials, Jiangsu Normal University, Xuzhou, 221116, China.

E-mail: gjchen@jsnu.edu.cn

[b] Department of Chemistry, The University of Tennessee, Knoxville, TN, 37996, USA

[c] Chemical Sciences Division, Oak Ridge National Laboratory, P.O. Box 2008, Oak Ridge, TN 37831, USA. E-mail: dais@ornl.gov

Experimental Section

Materials

Tetrakis[4-(1-imidazolyl)phenyl]methane (TIPM) was synthesized according to previous methods.[S1] 1-Phenyl-1H-imidazole (PhIM), 1,3-dibromo-2-propanol (DBPrOH), 1,3-dibromopropane (DBPr), epoxides and common solvents were commercially available and used without further purification.

Methods

Liquid-state ^{1}H and ^{13}C NMR spectra were measured with a Bruker DPX 500 spectrometer at ambient temperature in the solvent of D_2O using TMS as internal reference. Solid-state ^{13}C cross-polarization/magic angle spinning (CP/MAS) NMR spectra were carried out on a Bruker AVANCE III 600 spectrometer. The CHN elemental analysis was performed on an elemental analyzer Vario EL cube. Chemical compositions and states of the samples were determined by the X-ray photoelectron spectroscopy (XPS, Thermo ESCALAB 250Xi). Fourier transform infrared spectroscopy (FTIR) was recorded on a Bruker Vertex 80V FT-IR instrument (KBr discs) in the region 4000-400 cm^{-1}. Thermogravimetric analysis (TGA) was carried out with a TA Q50 instrument in nitrogen atmosphere at a heating rate of 10 $^{o}C\ min^{-1}$. X-ray diffraction (XRD) patterns were collected on the Bruker D8 Advance powder diffractometer using Ni-filtered Cu Ka radiation source at 40 kV and 20 mA, from 5 to 80^{o} with a scan rate of 0.2^{o} s^{-1}. Field emission scanning electron microscope (FESEM, Hitachi SU8010) accompanied by Energy dispersive X-ray spectrometry (EDS) was used to study the morphology and the elemental distribution. N_2 adsorption isotherms were measured at 77 K using a Quantachrome autosorb iQ2 analyzer, and the surface area of samples was calculated using the Brunauer-Emmett-Teller (BET) method and the pore size distribution was determined by the nonlocalized density functional theory (NLDFT) model, while the samples were degassed at 150°C for 10 h in high vacuum before analysis.

Synthesis of imidazolium ionic networks

Imidazolium ionic networks were prepared by the one-pot quaternization reaction between TIPM and DBPrOH or DBPr, as depicted in Scheme 1 and Scheme S1. In a typical run, TIPM (0.5 mmol, 0.2923 g) was homogeneously dispersed in CH_3CN (10 mL), and then DBPrOH (1 mmol, 0.2179 g) was added to the suspension solution. Subsequently, the above mixture solution was moved into a 25 mL Teflon-lined autoclave. The static reaction was taken place in a constant temperature oven at 100^{o}C for 48 h. After reaction, the solid product was collected by filtration and washed with N-Methyl pyrrolidone (NMP), water and ethanol for several times. After drying under

vacuum at 80°C for 12 h, a light-yellow powder solid (named IMIN-Br-OH) was obtained with the yield of 68%. Besides, the OH-free imidazolium ionic network (IMIN-Br, yield of 60%) was prepared by the replacement of DBPrOH with DBPr under similar synthetic conditions.

Elemental analysis calcd (wt%) for IMIN-Br-OH $[C_{43}H_{40}N_8Br_4O_2{\bullet}H_2O]_n$: C, 49.73, H, 4.08, N, 10.79; Found: C, 49.35, H, 5.01, N, 11.26. Elemental analysis calcd (wt%) for IMIN-Br $[C_{43}H_{40}N_8Br_4{\bullet}(4H_2O)]_n$: C, 48.70, H, 6.03, N, 10.57; Found: C, 46.85, H, 5.86, N, 10.61.

Synthesis of imidazolium ionic liquids

The control imidazolium ionic liquids were prepared by the quaternization reaction as follows (Scheme S2). First, 1-Phenyl-1H-imidazole (2 mmol, 0.2884 g), DBPr (1 mmol, 0.2019 g) and CH_3CN 10 mL was added into a 25 mL Teflon-lined autoclave with stirred for 20 minutes at room temperature. Then, the reaction was taken place at 100°C in a constant temperature oven for 48 h. After reaction, the white solid was immediately obtained by pouring the produced colourless solution into 50 mL ethyl acetate, and the mixture suspension was stirred for 1 h. The final suspension was filtered and subsequently washed with ethyl acetate (3×20 mL). After drying under vacuum at 80 °C for 12 h, a hygroscopic white solid (denoted as IL_1: D[PhIMPr]Br_2) was obtained with the yield of 86%. Besides, the OH-containing IL_2 D[PhIMPrOH]Br_2, a hygroscopic light brown solid with the yield of 77%, was similarly prepared by the reaction of 1-Phenyl-1H-imidazole with DBPrOH. The detailed NMR data are listed as follows, which are accordant with similar ionic liquids in previous literatures (*J. Organomet. Chem*., 2011, **696**, 3900-3905; *ChemCatChem*, 2015, **7**, 94-98; *Catal. Commun*., 2019, **124**, 118-122).

IL_1 D[PhIMPr]Br_2: ^{1}H NMR (400 MHz, d_6-DMSO) (Fig. S1A): δ=10.14 (NC*H*N, 2H), 8.37 (NC*H*CHN, 2H), 8.13 (NCHC*H*N, 2H), 7.82~7.54 (Ar-*H*, 10H), 4.41 (NCH_2, 4H), and 2.64 ppm (CH_2, 2H).^{13}C NMR (100 MHz, d_6-DMSO) (Fig. S1B): δ=136.31, 135.29, 130.71, 130.31, 123.90, 122.35, 121.65, 46.83, and 29.47 ppm.

IL_2 D[PhIMPrOH]Br_2: ^{1}H NMR (400 MHz, d_6-DMSO) (Fig. S2A): δ=9.98 (NC*H*N, 2H), 8.37 (NC*H*CHN, 2H), 8.07 (NCHC*H*N, 2H), 7.81~7.56 (Ar-*H*, 10H), 6.07 (O*H*, 1H), 4.61~4.54 (NCH_2C*H*OH, 3H), and 4.31~4.26 ppm (NCH_2, 2H). ^{13}C NMR (100 MHz, d_6-DMSO) (Fig. S2B): δ=136.53, 135.23, 130.76, 130.38, 124.65, 122.4, 121.56, 67.97, and 52.91 ppm.

Catalytic tests

The catalytic CO_2 fixation reaction was carried out using epichlorohydrin (ECH) as a typical substrate under mild conditions. In a typical run, ECH (2 mmol) and the catalyst IMIN-Br-OH (0.05 g) were placed in a Schlenk tube connected with a CO_2 balloon (0.1 MPa). After then, the mixture was stirred for desired time at the target

temperature. After reaction, ethyl acetate (2 mL) was added to the reaction mixture and stirred for 0.5 h, the solid catalyst was separated by centrifugation. The obtained filtrate was analyzed by gas chromatograph (GC) to afford the yield and selectivity of the product. For other substrates, the crude products were obtained by concentrating under reduced pressure and then were directly analyzed by ^{1}H NMR spectroscopy to determine the yields of cyclic carbonates. For the catalyst recycling experiments, the reaction was performed under the same reaction conditions each time using the recovered catalyst. The reusability of the catalyst was tested in five-run cycling experiments. The solid catalyst was collected by centrifuged, washed with ethanol, dried in vacuum and used to the next run.

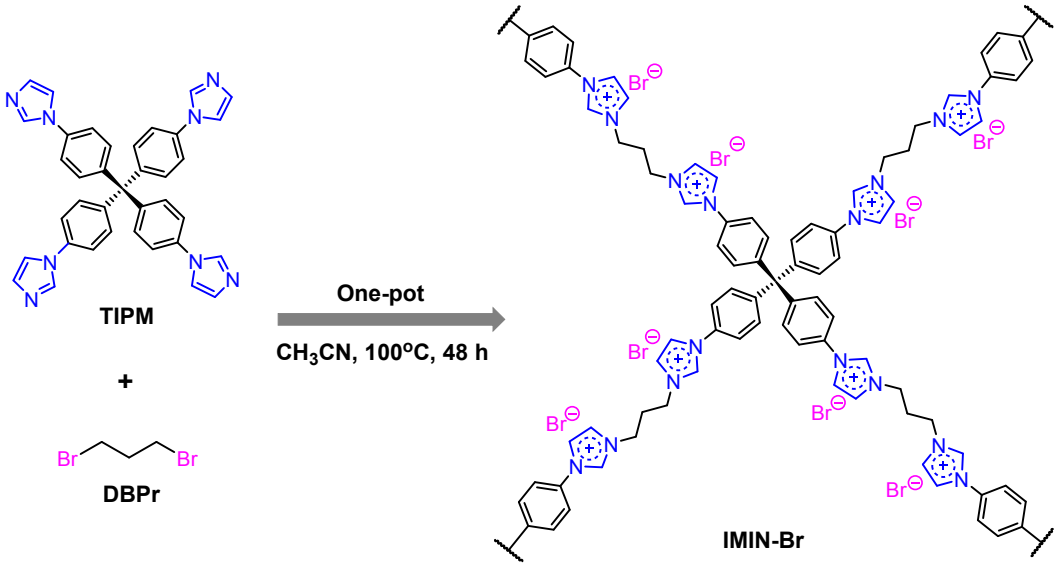

Scheme S1 Synthesis of the control hydroxyl-free imidazolium ionic network (IMIN-Br) by one-pot quaternization reaction between TIPM and with 1,3-dibromopropane (DBPr).

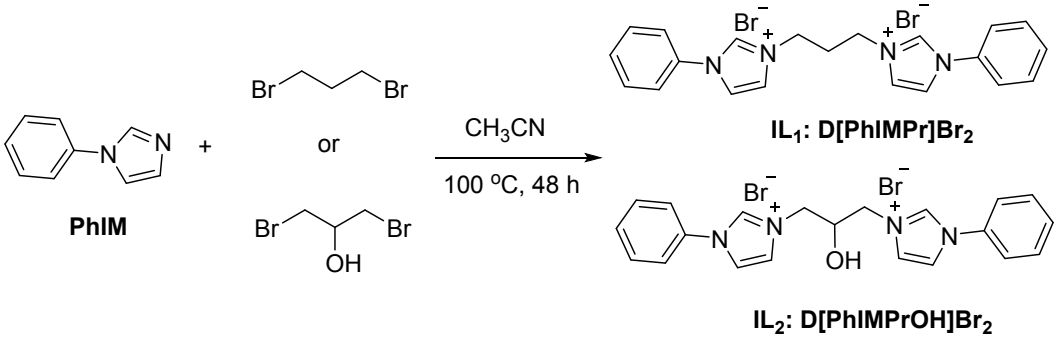

Scheme S2 Synthesis of the control hydroxyl-free and hydroxyl-containing imidazolium-based ionic liquids (IL_1 and IL_2).

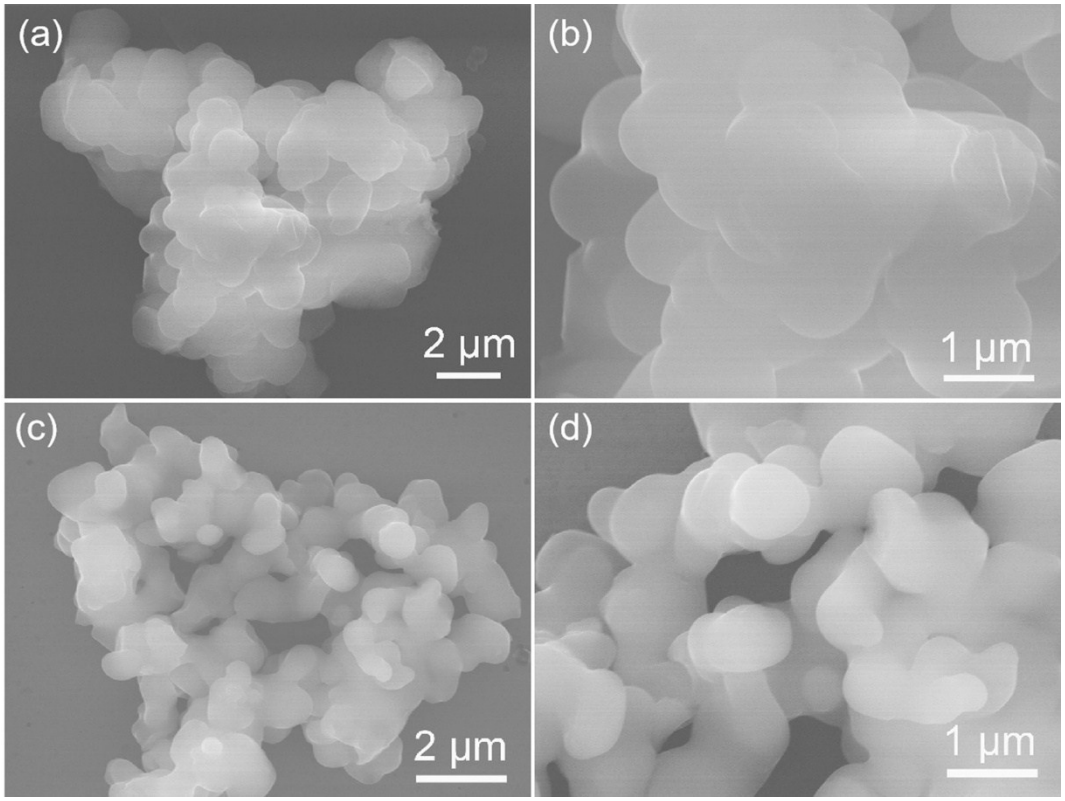

Fig. S1 Scanning electron microscope (SEM) images of (a, b) IMIN-Br and (c, d) IMIN-Br-OH.

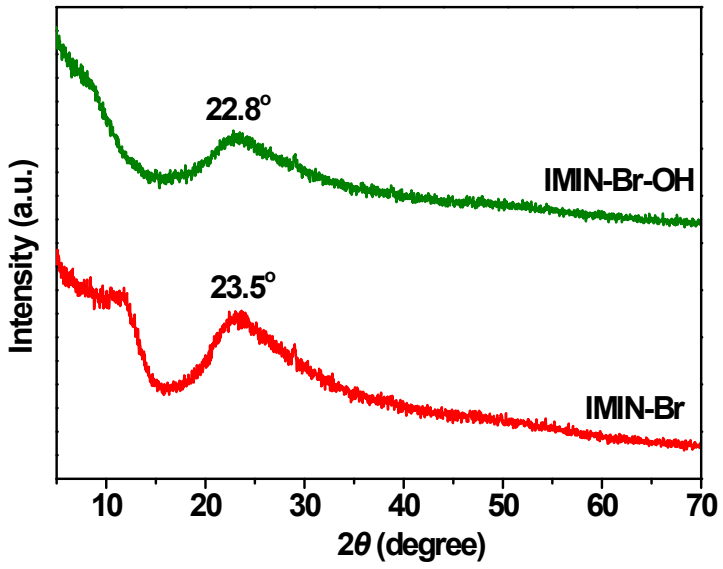

Fig. S2 X-ray diffraction patterns (XRD) patterns of IMIN-Br-OH and IMIN-Br.

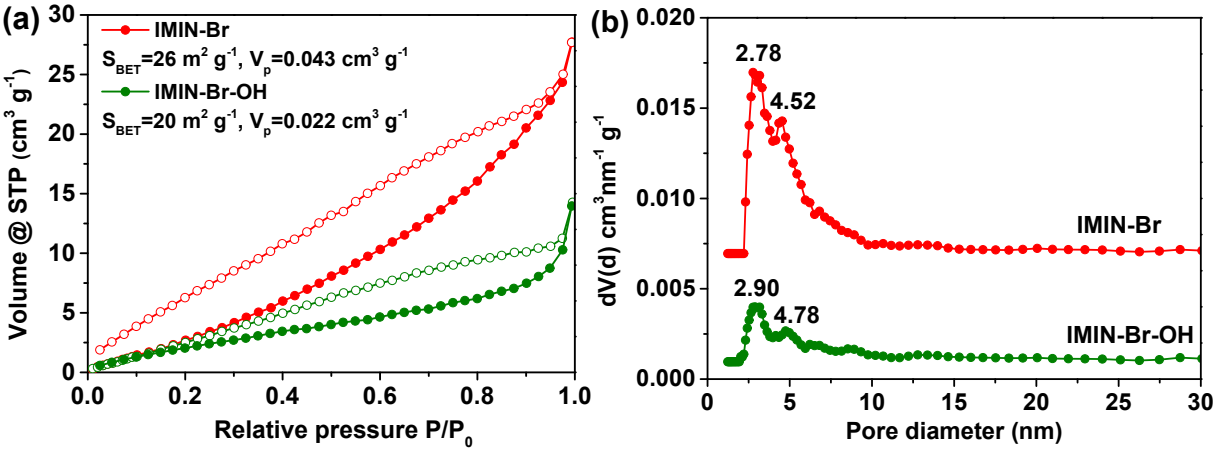

Fig. S3 (a) N_2 adsorption-desorption isotherms, (b) NLDFT pore size distributions of IMIN-Br and IMIN-Br-OH.

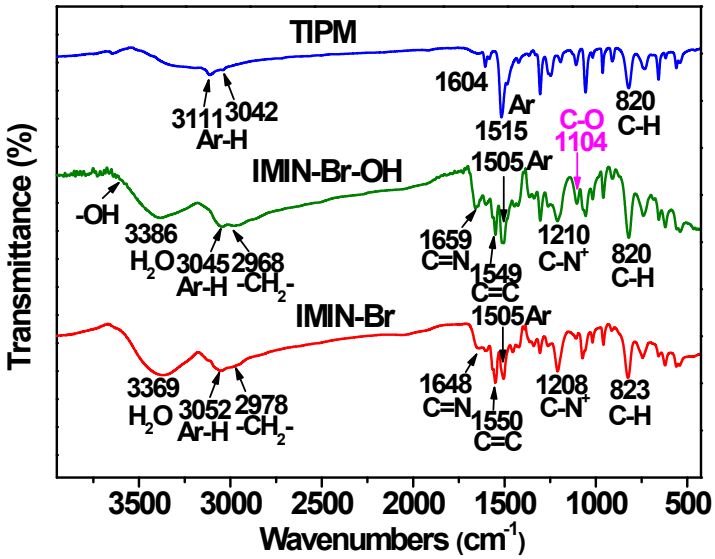

Fig. S4 FTIR spectra of TIPM, IMIN-Br-OH and IMIN-Br.

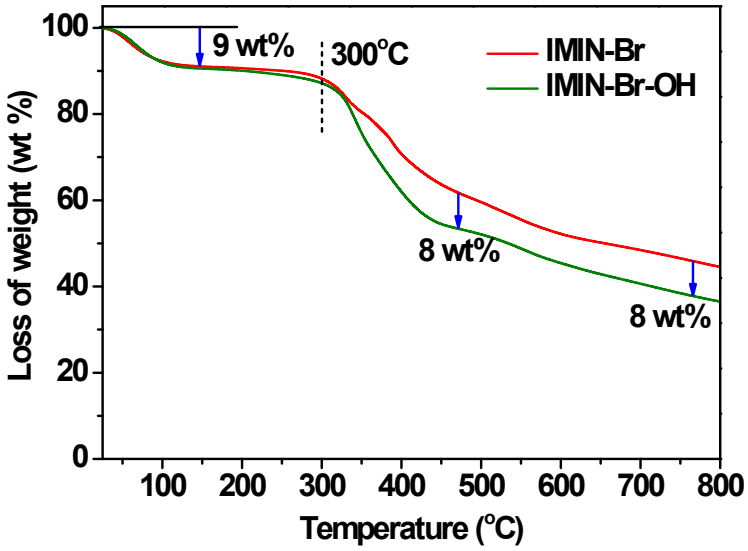

Fig. S5 Thermogravimetric analysis (TGA) curves of IMIN-Br and IMIN-Br-OH under N_2 atmosphere.

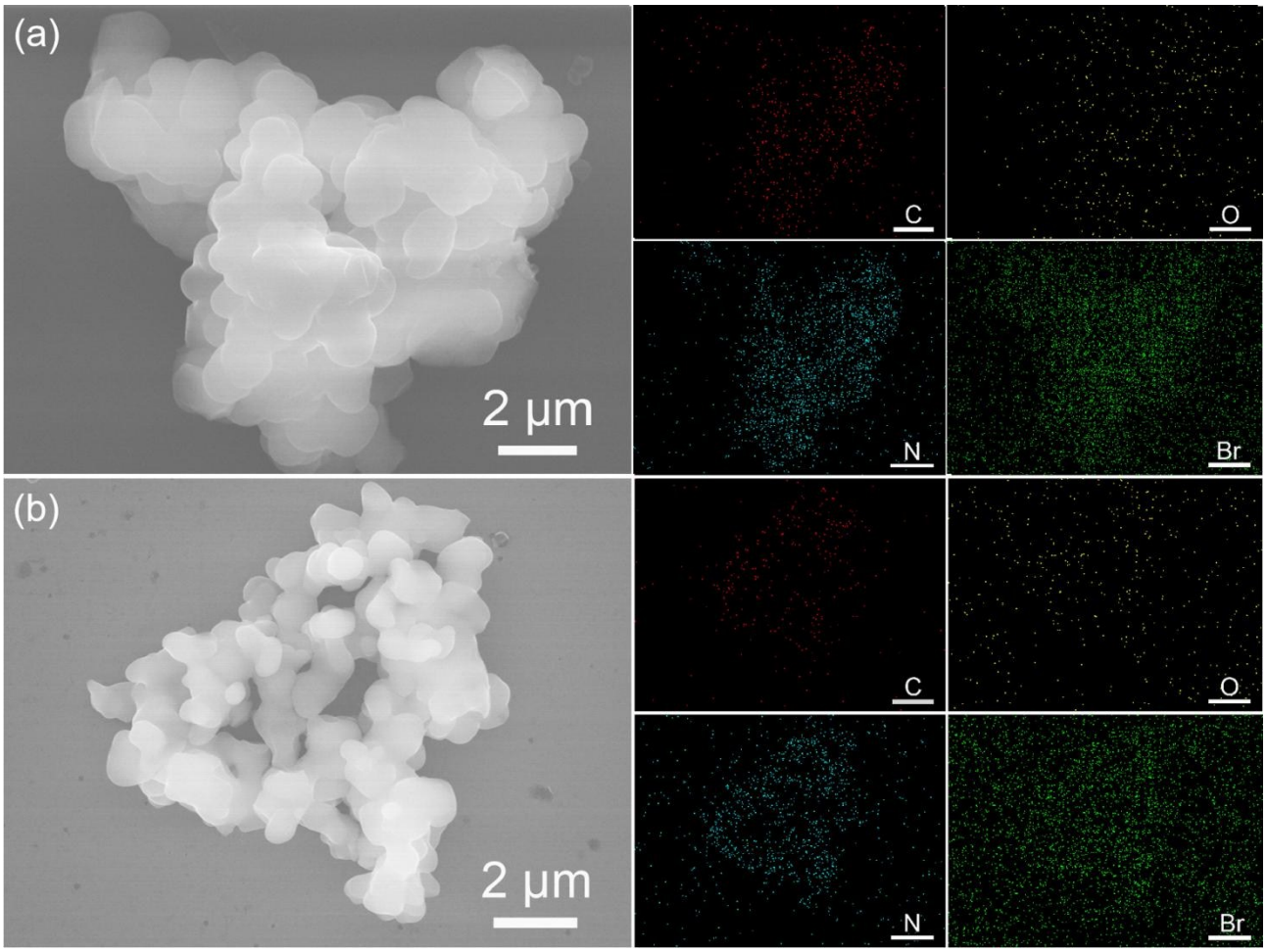

Fig. S6 Energy-dispersive X-ray spectrometry (EDS) elemental mapping images of (a) IMIN-Br and (b) IMIN-Br-OH for C, O, N and Br at the SEM mode.

Table S1 Cycloaddition of CO_2 with ECH catalyzed by the IMINs and the control ILs under different conditions.[a]

Entry	Catalyst	T (°C)	t (h)	Yield (%) [b]	Selectivity (%) [b]	TOF value (h^{-1}) [c]
1	IMIN-Br	60	48	98	99	0.269
2	IMIN-Br-OH	60	48	99	99	0.257
3	IMIN-Br	50	48	70	99	0.192
4	IMIN-Br-OH	50	48	97	99	0.251
5	IMIN-Br	40	72	80	99	0.147
6	IMIN-Br-OH	40	72	99	99	0.171
7	IMIN-Br	30	120	56	99	0.062
8	IMIN-Br-OH	30	120	90	99	0.093
9	D[PhIMPr]Br_2	40	72	92	99	0.157
10	D[PhIMPrOH]Br_2	40	72	99	99	0.174

[a] Reaction conditions: ECH (2 mmol), CO_2 balloon (0.1 MPa), the catalyst (0.04 g), temperature (T=30~60°C), time (t=48~120 h); [b] Yield and selectivity of the cyclic carbonate were determined by GC and ^{1}H NMR. [c] Turnover frequency (TOF) = [mmol (product)] / [mmol (IM ionic content in the catalyst) × reaction time (h)]. Imidazolium (IM) ionic contents (3.79 mmol g^{-1} for IMIN-Br and 4.02 mmol g^{-1} for IMIN-Br-OH) were calculated by the elemental analysis results.

Table S2 The detailed comparisons of catalytic activities over metal-free IL-derived ionic polymers and ionic polymers with HBD groups for CO_2 fixation with ECH without any co-catalysts.*

Catalyst	*P* (MPa)	*T* (°C)	*t* (h)	Yield (%)	Ref.
PCP-Cl	3	100	12	98	S2
F-PIL-Br	1	120	9	93	S3
PIM2	1	130	4	92	S4
IT-POP-1	1	120	10	99	S5
poly-imidazoliums	1	110	2	94	S6
POM3-IM	1	120	8	90	S7
cCTF-500	1	90	12	95	S8
FIP-Im	1	80	10	99	S9
3-IPMP-EtI	1	90	5	90	S10
UIIP	1	90	2	99	S11
CCTF-350	0.1	120	24	93.1	S12
PDMBr	0.1	120	12	91.3	S13
IP3	0.1	100	24	99	S14
PIP-Bn-Cl	0.1	100	3	99	S15
COP-222	0.1	100	24	99	S16
PDBA-Cl-SCD	0.1	90	6	99.3	S17
PGDBr-5-2OH	0.1	70	24	91	S18
HIP-Br-2	0.1	70	96	90	S19
V-PCIF-Br	0.1	80	72	97	S20
V-iPHP-1	0.1	60	72	99	S21
IM-iPHP-2	0.1	60	72	99	S22
PPS-mOH-Bn	0.1	50	72	78	S23
POF-PNA-Br	0.1	40	48	94.1	S24
IMIN-Br-OH	**0.1**	**50**	**48**	**97**	**This work**
IMIN-Br-OH	**0.1**	**40**	**72**	**99**	**This work**
IMIN-Br-OH	**0.1**	**30**	**120**	**90**	**This work**

* It should be pointed out that different catalysts were evaluated under different conditions. Thus, it is difficult to directly compare the activity between different catalytic systems. The above represented catalytic activities should be considered in a reasonable comparison.

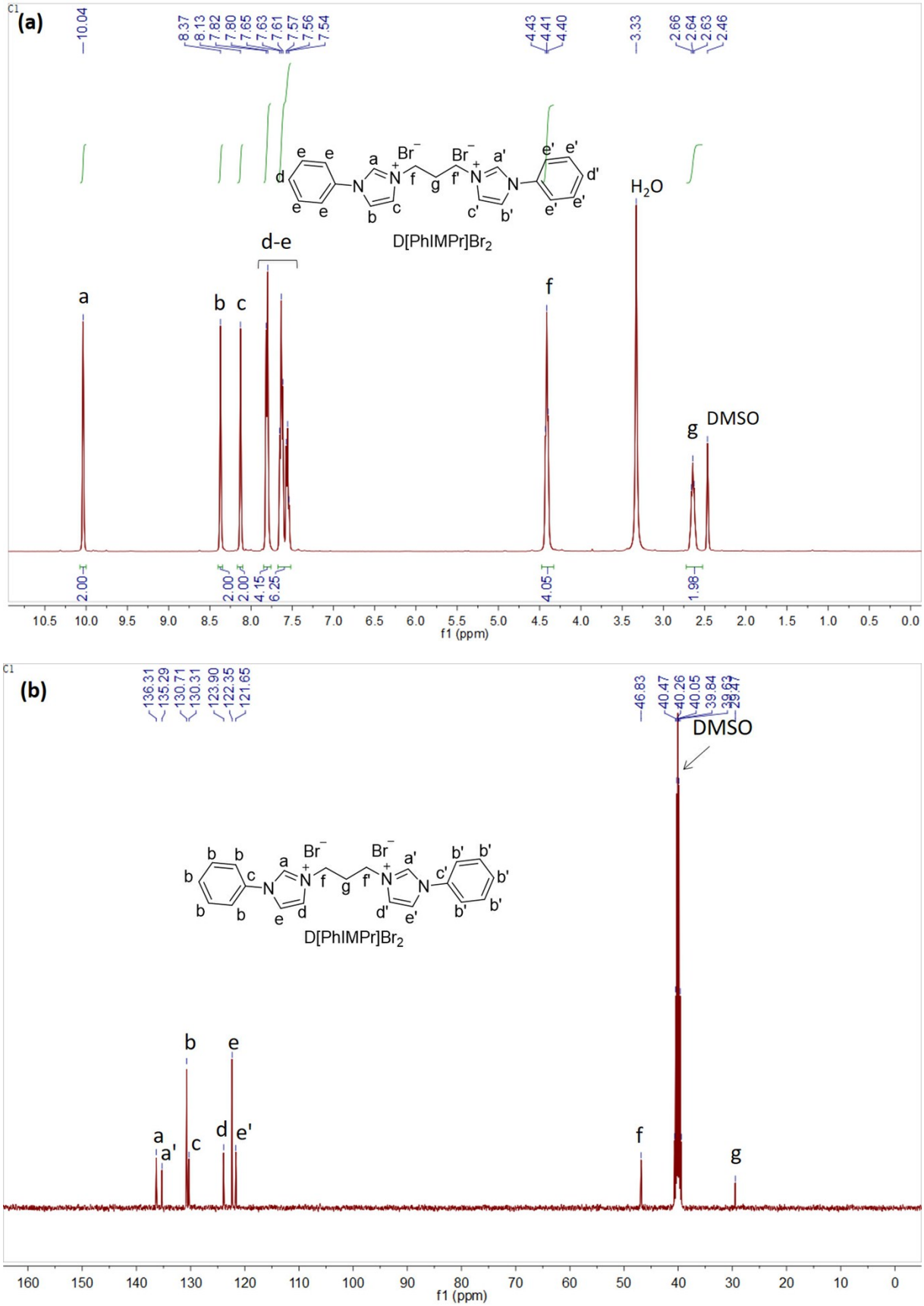

Fig. S7 (a) ^{1}H NMR and (b) ^{13}C NMR of D[PhIMPr]Br_2 using the solvent of d_6-DMSO.

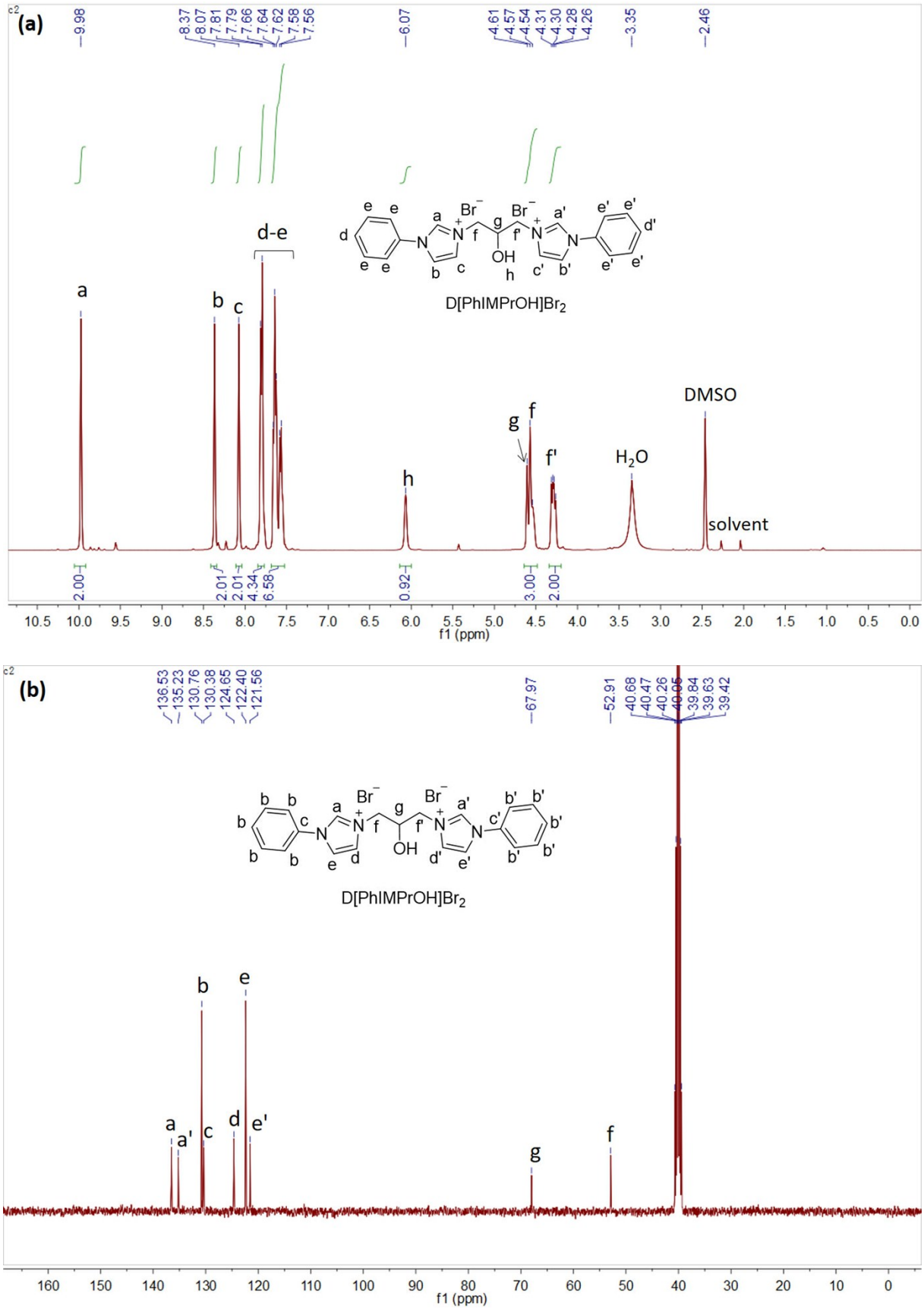

Fig. S8 (a) ^{1}H NMR and (b) ^{13}C NMR of D[PhIMPrOH]Br_2 using the solvent of d_6-DMSO.

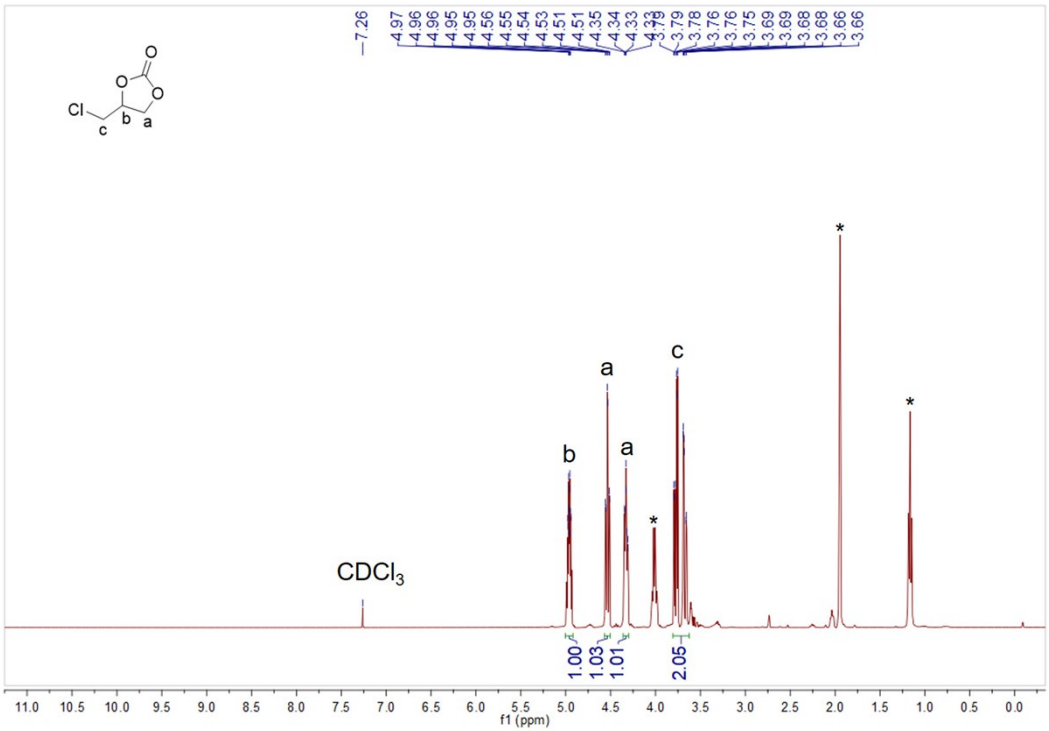

Fig. S9 ^{1}H NMR spectrum of 4-(chloromethyl)-1,3-dioxolan-2-one (400 MHz, $CDCl_3$): δ=5.00~4.92 (1H, CH), 4.53 (1H, CH_2), 4.36~4.30 (1H, CH_2), 3.81~3.63 ppm (2H, CH_2).

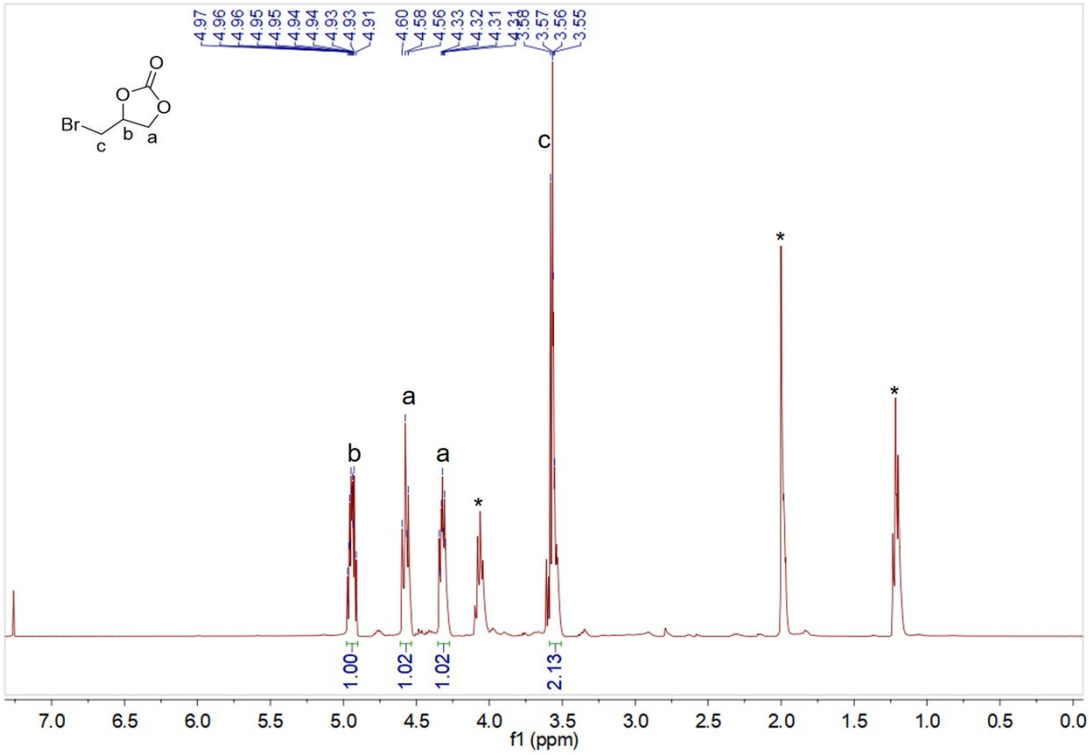

Fig. S10 ^{1}H NMR spectrum of 4-(bromomethyl)-1,3-dioxolan-2-one (400 MHz, $CDCl_3$): δ=4.97~4.01 (1H, CH), 4.60~4.56 (1H, CH_2), 4.33~4.31 (1H, CH_2), 3.58~3.55 ppm (2H, CH_2).

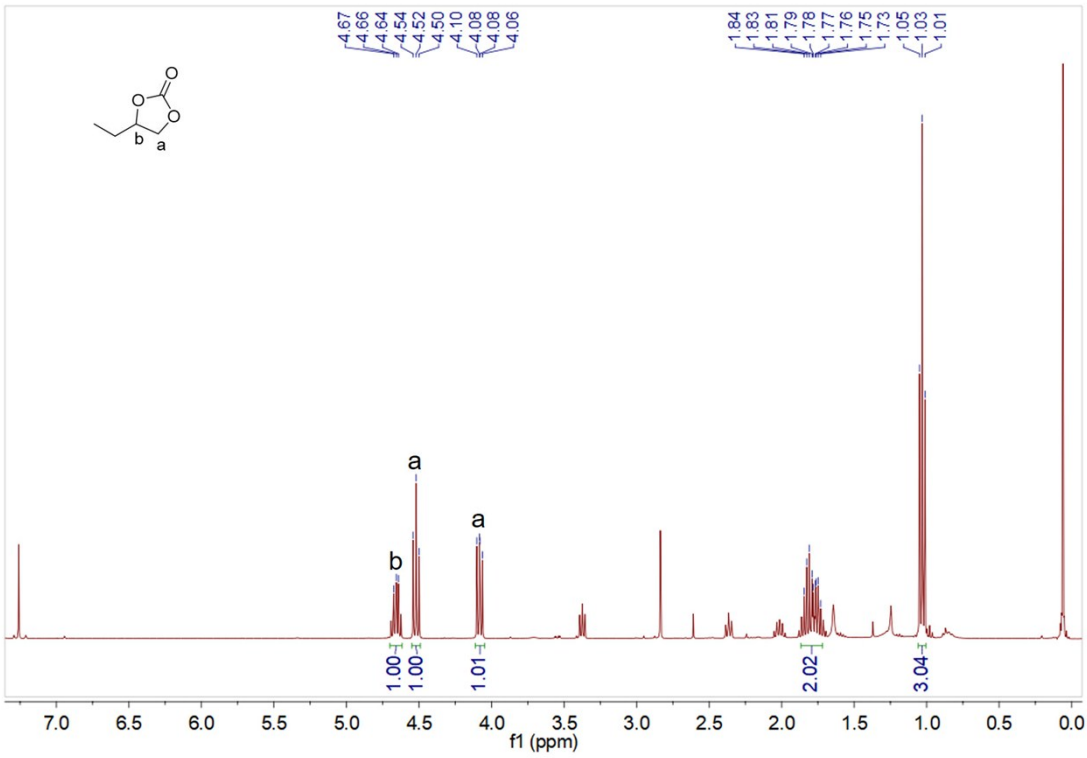

Fig. S11 ^{1}H NMR spectrum of 4-ethyl-1,3-dioxolan-2-one (400 MHz, $CDCl_3$): δ=4.70~4.62 (1H, CH_2), 4.52 (1H, CH_2), 4.08 (1H, CH_2), 1.87~1.72 (2H, CH_2), 1.03 ppm (3H, CH_3).

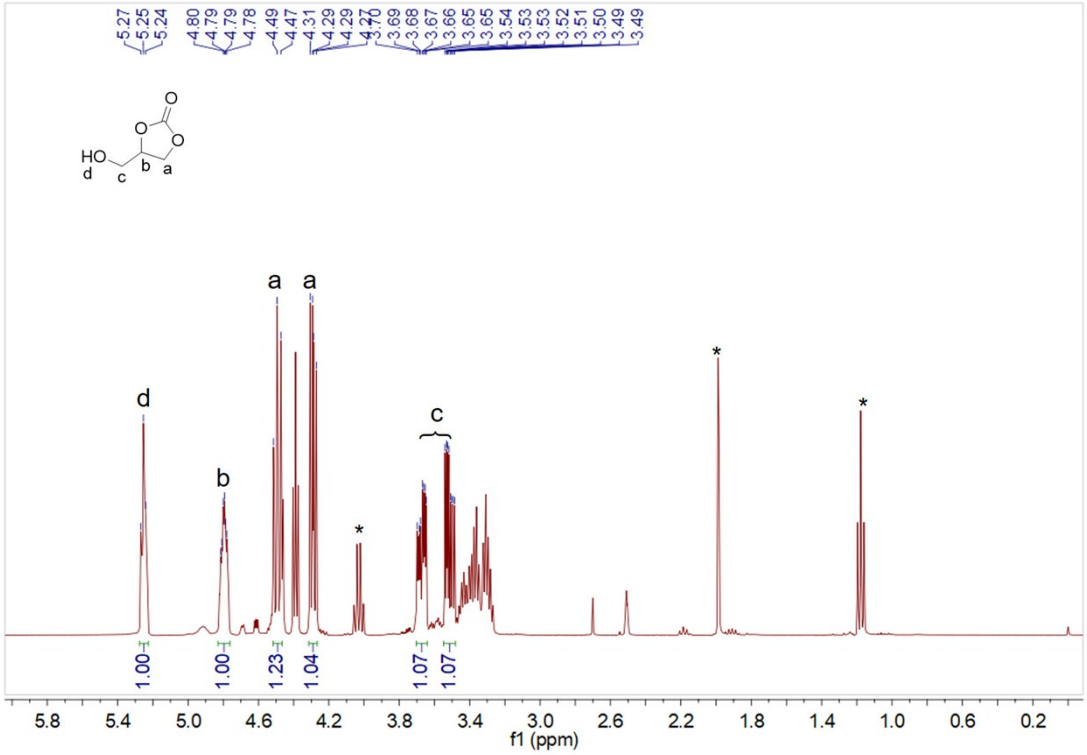

Fig. S12 ^{1}H NMR spectrum of 4-(hydroxymethyl)-1,3-dioxolan-2-one (400 MHz, d_6-DMSO): 5.25 (1H, OH), 4.8 (1H, OCH), 4.52~4.47 (1H, CH_2O), 4.29 (1H, CH_2O), 3.70~3.64 (1H, CH_2OH), 3.51 ppm (1H, CH_2OH).

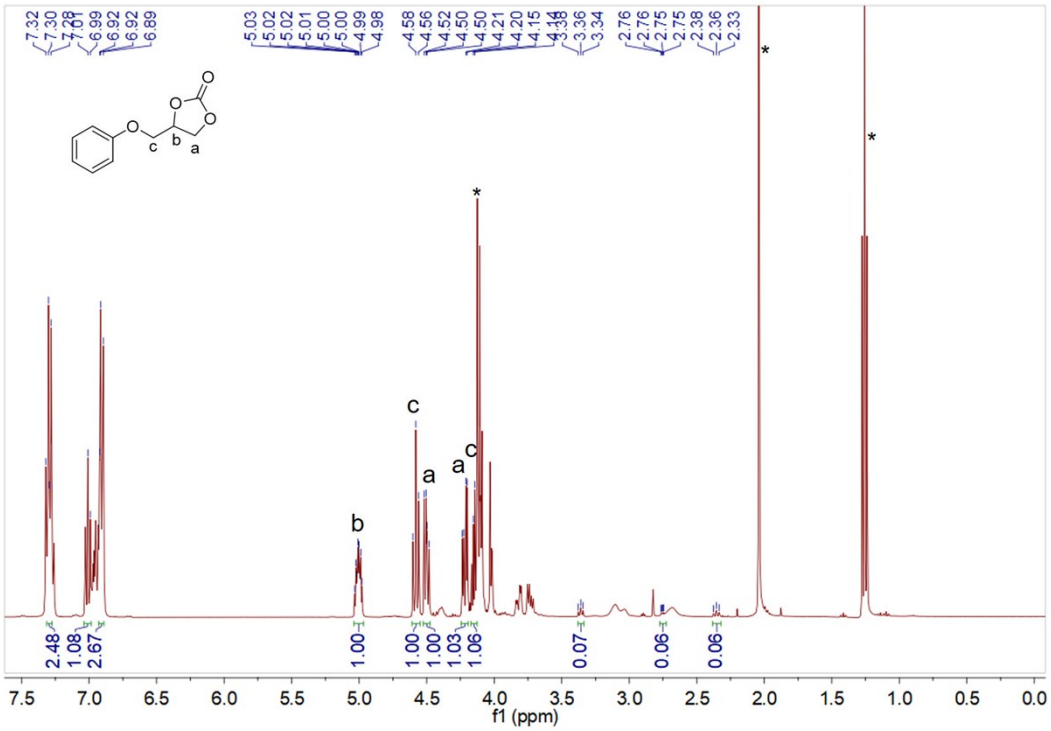

Fig. S13 ^{1}H NMR spectrum of 4-(phenoxymethyl)-1,3-dioxolan-2-one (400 MHz, $CDCl_3$): δ=7.31~7.27 (2H, CH), 7.00 (1H, CH), 6.93~6.89 (2H, CH), 5.04~4.97 (1H, CH), 4.58 (1H, CH_2), 4.50 (1H, CH_2), 4.22 (1H, CH_2), 4.15 ppm (1H, CH_2).

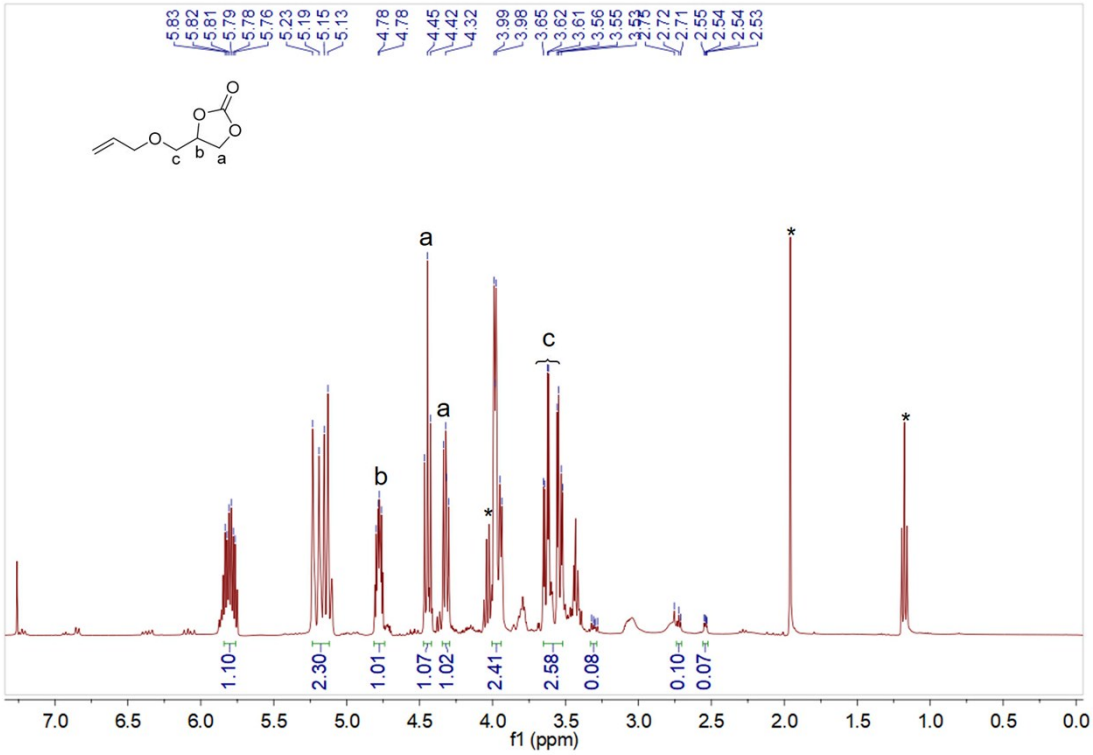

Fig. S14 ^{1}H NMR spectrum of allyloxymethyl-1,3-dioxolan-2-one (400 MHz, $CDCl_3$): δ=5.84~5.76 (1H, CH), 5.18 (2H, CH_2), 4.78 (1H, CH), 4.45 (1H, CH_2), 4.32 (1H, CH_2), 3.97 (2H, CH_2), 3.59 ppm (2H, CH_2).

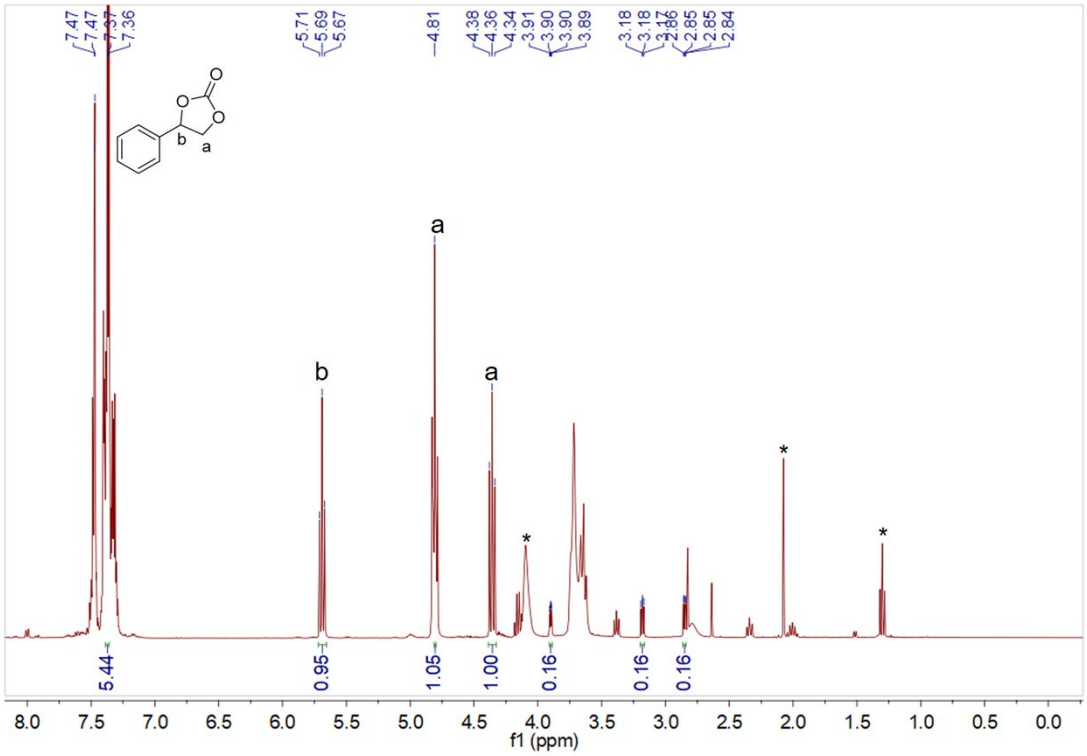

Fig. S15 ^{1}H NMR spectrum of 4-phenyl-1,3-dioxolan-2-one (400 MHz, $CDCl_3$): δ=7.37 (5H, CH), 5.69 (1H, CH_2), 4.81(1H, CH_2), 4.36 ppm (1H, CH_2).

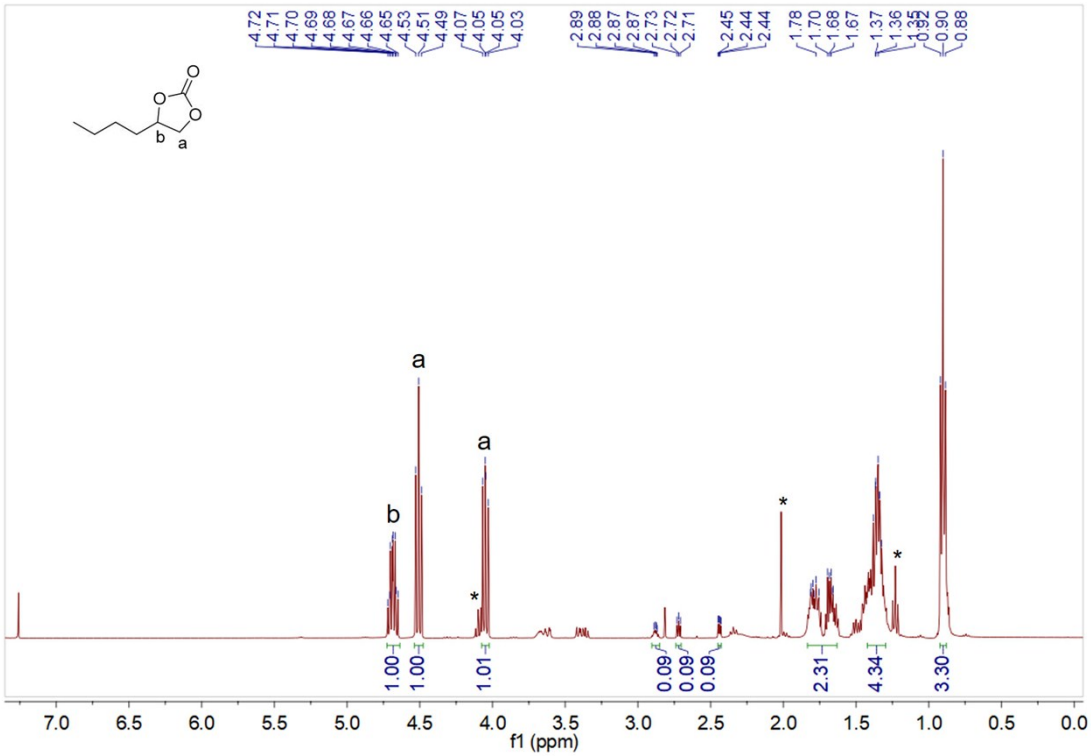

Fig. S16 ^{1}H NMR spectrum of 4-butyl-1,3-dioxolan-2-one (400 MHz, $CDCl_3$): δ=4.69 (1H ,CH_2), 4.51 (1H, CH_2), 4.05 (1H, CH_2), 1.83~1.63 (2H, CH_2), 1.42~1.30 (4H, CH_2), 0.90 ppm (3H, CH_3).

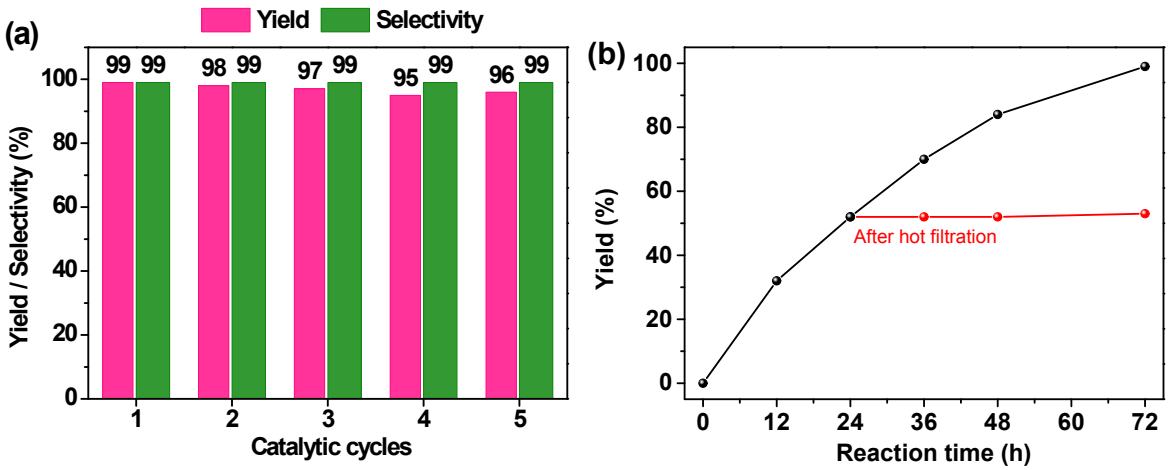

Fig. S17 (a) A five-cycle assessment in the catalytic reusability of IMIN-Br-OH for the CO_2 conversion with ECH. (b) Hot filtration test for the CO_2 conversion with ECH using the IMIN-Br-OH catalyst. Reaction conditions: ECH (2 mmol), CO_2 pressure (0.1 MPa), the catalyst (0.04 g), 40°C, 72 h.

As shown in Fig. S17, a five-cycle test was carried out to evaluate the recyclability of the heterogeneous catalyst IMIN-Br-OH in the cycloaddition of CO_2 with ECH under mild conditions. After five runs, the catalyst shows no obvious decrease in both the yield and selectivity, attributing to the well-preserved chemical composition and structural morphology of the recovered catalyst (see FTIR in Fig. S18 and SEM images in Fig. S19). Hot filtration test was also employed to ensure the heterogeneous nature of IMIN-Br-OH and check whether there existed the homogeneous active species after removing the solid catalyst. In a typical hot filtration test, the reaction was stopped by an immediate hot filtration to remove the solid catalyst IMIN-Br-OH from the reaction system at the reaction time of 24 h. With the reaction of the filtrate solution going on, the yield no longer increases with the reaction time as shown in the red line in Fig. S17b. Besides, no leaching of imidazolium ILs was detected from the filtrate by ^{1}H NMR or the concentrated solution by elemental analysis. The above results demonstrate the good recyclability and the heterogeneous nature of IMIN-Br-OH.

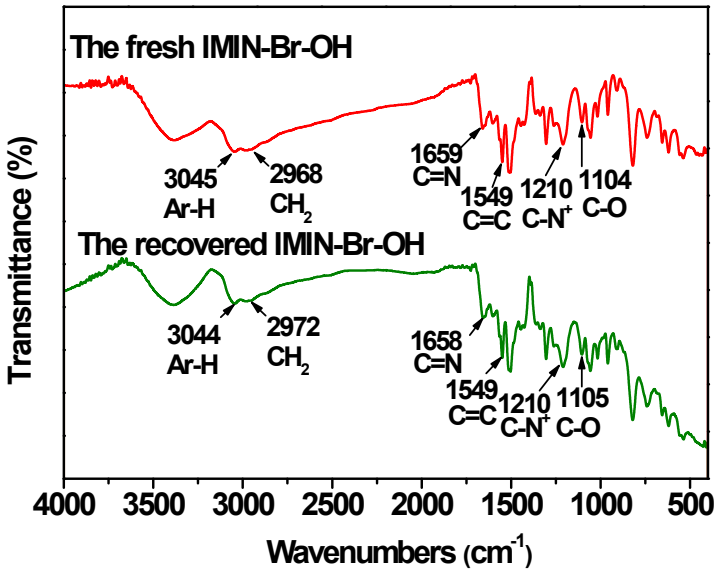

Fig. S18 FTIR of the fresh catalyst IMIN-Br-OH and the recovered catalyst IMIN-Br-OH.

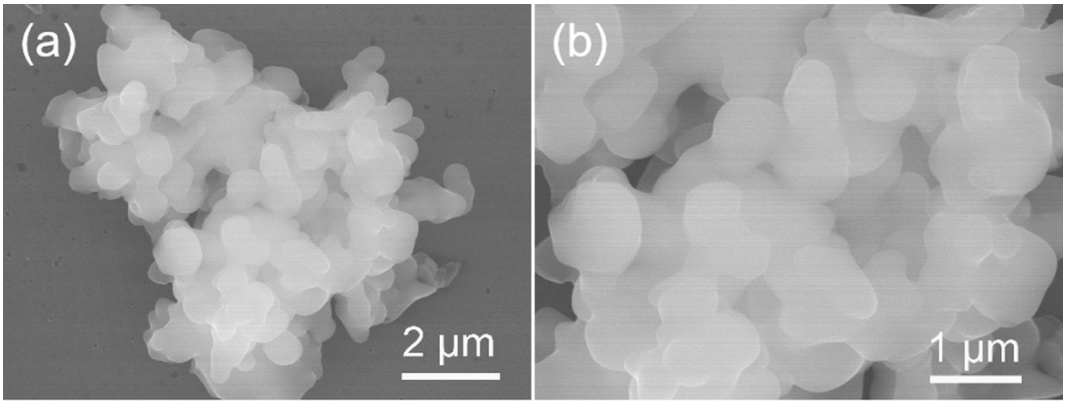

Fig. S19 SEM images of the recovered catalyst IMIN-Br-OH.

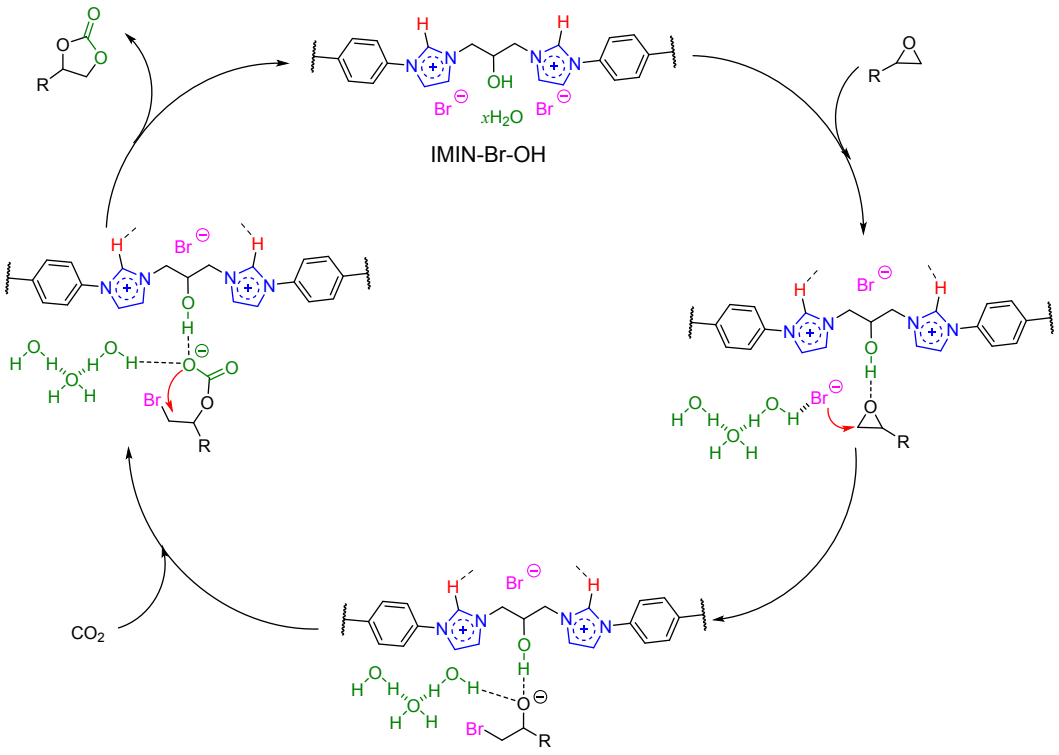

Scheme S3 A plausible synergistic catalytic mechanism for the CO_2 fixation with epoxides promoted by multi-hydrogen-bond donors and Br^- anions in the catalyst IMIN-Br-OH.

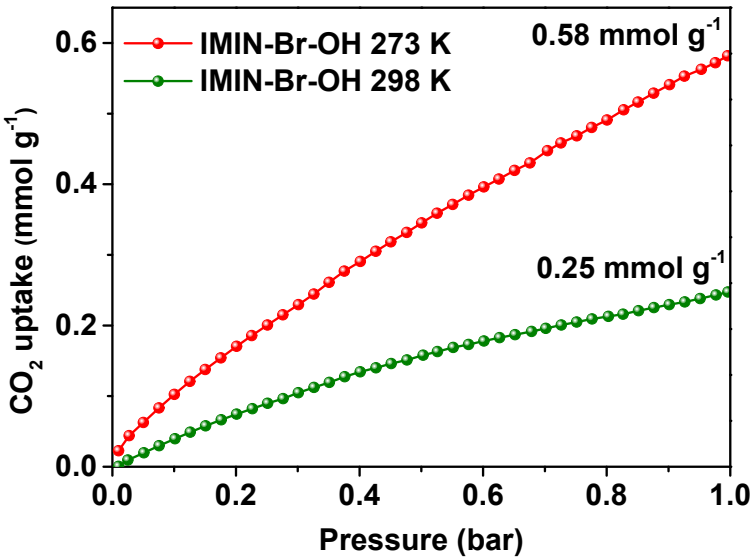

Fig. S20 CO_2 adsorption isotherms of IMIN-Br-OH collected up to 1.0 bar at 273 K and 298 K.

The CO_2 adsorption isotherms of IMIN-Br-OH were collected up to 1.0 bar at 273 K and 298 K (Fig. S20) , giving moderate CO_2 adsorption capacities (0.58 mmol g^{-1} at 273 K and 0.25 mmol g^{-1} at 298 K). The moderate CO_2 adsorption capacities of IMIN-Br-OH make for the interaction between CO_2 molecules, substrates, and catalytic active sites.

References

S1 J. Choi, H. Y.Yang, H. J. Kim and S. U. Son, *Angew. Chem. Int. Ed.*, 2010, **49**, 7718-7722.

S2 O. Buyukcakir, S. H. Je, D. S. Choi, S. N. Talapaneni, Y. Seo, Y. Jung, K. Polychronopoulouc and A. Coskun, *Chem. Commun*., 2016, **52**, 934-937.

S3 Z.-Z. Yang, Y. Zhao, G. Ji, H. Zhang, B. Yu, X. Gao and Z. Liu, *Green Chem*., 2014, **16**, 3724-3728.

S4 Y. Wang, J. Nie, C. Lu, F. Wang, C. Ma, Z. Chen and G. Yang, *Micropor. Mesopor. Mater*., 2020, **292**, 109751.

S5 H. Zhong, Y. Su, X. Chen, X. Li, R. Wang, *ChemSusChem*, 2017, **10**, 4855-4863.

S6 J. Wang, J. Leong and Y. Zhang, *Green Chem*., 2014, **16**, 4515-4519.

S7 J. Wang, W. Sng, G. Yi and Y. Zhang, *Chem. Commun*., 2015, **51**, 12076-12079.

S8 O. Buyukcakir, S. H. Je, S. N. Talapaneni, D. Kim and A. Coskun, *ACS Appl. Mater. Interfaces*, 2017, **9**, 7209-7216.

S9 Y. Chen, R. Luo, J. Bao, Q. Xu, J. Jiang, X. Zhou and H. Ji, *J. Mater. Chem. A*, 2018, **6**, 9172-9182.

S10 W. Zhang, Y. Mei, P. Wu, H.-H. Wu and M.-Y. He, *Catal. Sci. Technol*., 2019, **9**, 1030-1038.

S11 M. A. Ziaee, Y. Tang, H. Zhong, D. Tian and R. Wang, *ACS Sustainable Chem. Eng*., 2019, **7**, 2380-2387.

S12 T.-T. Liu, R. Xu, J.-D. Yi, J. Liang, X.-S. Wang, P.-C. Shi, Y.-B. Huang and R. Cao, *ChemCatChem*, 2018, **10**, 2036-2040.

S13 X. Wang, Y. Zhou, Z. Guo, G. Chen, J. Li, Y. Shi, Y. Liu and J. Wang, *Chem. Sci*., 2015, **6**, 6916-6924.

S14 W. Zhong, F. D. Bobbink, Z. Fei and P. J. Dyson, *ChemSusChem*, 2017, **10**, 2728-2735.

S15 Q. Sun,Y. Jin, B. Aguila, X. Meng, S. Ma and F.-S. Xiao, *ChemSusChem*, 2017, **10**, 1160-1165.

S16 S. Subramanian, J. Oppenheim, D. Kim, T. S. Nguyen,W. M.H. Silo, B. Kim, W. A. Goddard III and C. T. Yavuz, Chem (2019), https://doi.org/10.1016/j.chempr.2019.10.009.

S17 Y. Xie, Q. Sun, Y. Fu, L. Song, J. Liang, X. Xu, H. Wang, J. Li, S. Tu, X. Lu and J. Li, *J. Mater. Chem. A*, 2017, **5**, 25594-25600.

S18 Z. Guo, Q. Jiang, Y. Shi, J. Li, X. Yang, W. Hou, Y. Zhou and J. Wang, *ACS Catal.*, 2017, **7**, 6770-6780.

S19 J. Li, D. Jia, Z. Guo, Y. Liu, Y. Lyu, Y. Zhou and J. Wang, *Green Chem.*, 2017, **19**, 2675-2686.

S20 G. Chen, X. Huang, Y. Zhang, M. Sun, J. Shen, R. Huang, M. Tong, Z. Long and X. Wang, *Chem. Commun*., 2018, **54**, 12174-12177.

S21 Y. Zhang, K. Liu, L. Wu, H. Zhong, N. Luo, Y. Zhu, M. Tong, Z. Long and G. Chen, *ACS Sustainable Chem.*

Eng., 2019, **7**, 16907-16916.

S22 G. Chen, Y. Zhang, J. Xu, X. Liu, K. Liu, M. Tong and Z. Long, *Chem. Eng. J.*, 2020, **381**, 122765.

S23 K. Hu, Y. Tang, J. Cui, Q. Gong, C. Hu, S. Wang, K. Dong, X. Meng, Q. Sun and F.-S. Xiao, *Chem. Commun*., 2019, **55**, 9180-9183.

S24 D. Ma, K. Liu, J. Li and Z. Shi, *ACS Sustainable Chem. Eng*., 2018, **6**, 15050-15055.